Three-Body Ampli cation of Photon Heat Tunneling Supplementary Material

Riccardo Messina, Mauro Antezza, Philippe Ben-Abdallah

Three-Body Amplification of Photon Heat Tunneling

Riccardo Messina,[1,*] Mauro Antezza,[2,3,†] and Philippe Ben-Abdallah[1,‡]

[1]*Laboratoire Charles Fabry, UMR 8501, Institut d'Optique, CNRS, Université Paris-Sud 11, 2 Avenue Augustin Fresnel, 91127 Palaiseau Cedex, France*

[2]*Laboratoire Charles Coulomb UMR 5221, Université Montpellier 2, F-34095 Montpellier, France*

[3]*Laboratoire Charles Coulomb UMR 5221, CNRS, F-34095 Montpellier, France*

Resonant tunneling of surface polaritons across a subwavelength vacuum gap between two polar or metallic bodies at different temperatures leads to an almost monochromatic heat transfer which can exceed by several orders of magnitude the far-field upper limit predicted by Planck's blackbody theory. However, despite its strong magnitude, this transfer is very far from the maximum theoretical limit predicted in the near field. Here we propose an amplifier for the photon heat tunneling based on a *passive relay* system intercalated between the two bodies, which is able to partially compensate the intrinsic exponential damping of energy transmission probability thanks to three-body interaction mechanisms. As an immediate corollary, we show that the exalted transfer observed in the near field between two media can be exported at larger separation distances using such a relay. Photon heat tunneling assisted by three-body interactions enables novel applications for thermal management at nanoscale, near-field energy conversion and infrared spectroscopy.

Two bodies held at different temperatures and separated by a vacuum gap exchange in permanence heat throughout the thermal electromagnetic field they radiate. At a long separation distance (i.e., in the far field) this exchange of energy results exclusively from propagative photons emitted by these sources. The blackbody limit given by the famous Stefan-Boltzmann law sets the maximum heat flux these media can exchange. However, at subwavelength distances (i.e., in near-field regime) the situation radically changes. Indeed, at this scale, evanescent photons which remain confined near the surface of materials are the main contributors to transfer and they participate via tunneling through the vacuum gap [1–8]. A significant heat-flux increase results from this transport. In the presence of resonant surface modes such as surface plasmons or surface polaritons, collective electron or partial charge oscillations coupled to light waves at the surface, the radiative-heat exchanges can even drastically surpass by several orders of magnitude the prediction of Planck's blackbody theory. This discovery opened new possibilities for the development of innovative technologies for nanoscale thermal management, such as near-field energy conversion (thermophotovoltaic conversion devices [9,10]), heating assisted data storage (plasmon assisted nanophotolitography [11]) or IR sensing and spectroscopy [12,13].

Recent theoretical developments [14,15] have established that the nanoscale heat transfer between two media separated by a distance d can be revisited using the same concepts as in mesoscopic physics of charge transport. The first step is the expression of the distance-dependent heat flux $\varphi(d)$ under the form of a spectral decomposition $\varphi(d) = \int_0^{+\infty} \frac{d\omega}{2\pi} \phi(\omega, d)$. Hence, the monochromatic near-field heat flux transferred between two media at temperatures T_1 and T_2 is described in a Landauer-like formalism [14–17] as the sum over all modes

$$\phi(\omega, d) = \hbar\omega n_{12}(\omega) \sum_p \int \frac{d^2\mathbf{k}}{(2\pi)^2} \mathcal{T}_p(\omega, \mathbf{k}, d) \qquad (1)$$

of the energy $\hbar\omega$ of each mode $(\omega, \mathbf{k}, p)$ [identified by the frequency ω, the transverse wave vector $\mathbf{k} = (k_x, k_y)$ and the polarization p], times a transmission probability $\mathcal{T}_p(\omega, \mathbf{k}, d)$ through the separation gap (assuming values between 0 and 1), with $n_{ij}(\omega) = n(\omega, T_i) - n(\omega, T_j)$, $n(\omega, T) = (e^{\hbar\omega/k_B T} - 1)^{-1}$ being the distribution function inside the reservoir of modes at temperature T. Analysis of arbitrary systems has revealed a rather small efficiency of transfer coefficient for each exchange channel even in the presence of resonant surface modes such as surface polaritons. In this situation the total number of channels (i.e., number of modes) contributing to the heat transfer per unit of surface is set by the position of the cutoff for the transverse component of wave vector $k_c \simeq \log[2/\sqrt{\mathrm{Im}(\varepsilon_1)\mathrm{Im}(\varepsilon_2)}]/d$ [15,18], where $\mathrm{Im}(\varepsilon_i)$ denotes the imaginary part of the dielectric permittivity of the material i ($i = 1, 2$). This allows us to estimate two fundamental limits [14] $\phi_{\max} = k_B^2(T_1^2 - T_2^2)k_c^2/6\hbar$ and $h_{\max} = g_0 k_c^2/\pi$ ($g_0 = \pi^2 k_B^2 T/3h$ is the quantum of thermal conductance at temperature T), respectively, for the monochromatic flux and total heat transfer coefficient between two media. However, these limits are intrinsic to two-body systems but are not universals in general. In the

present Letter we describe heat transfer in three-body systems and we highlight the concept of three-body amplification of heat flux exchanged at nanoscale between two media. In addition we propose a device based on an intermediate *passive relay*, which is able to increase the number of coupled modes. This investigation belongs to the vast category of few-body problems whose richness has been largely explored in atomic physics, quantum chemistry, and celestial mechanics. Recently, interesting effects have been theoretically discussed in the context of heat transfer [19,20].

We consider two parallel slabs identified for convenience by the indexes $i = 1$ and $i = 3$, as shown in Fig. 1(a). Each slab has a finite thickness, whereas its transverse extension is much larger than the distance between the slabs, so that they can be considered infinite with respect to the xy plane. We compare this system to a configuration in which a third slab, labeled with $i = 2$ and having thickness δ, is placed between slabs 1 and 3 [see Fig. 1(b)]. The system is placed in both cases in a stationary thermodynamical configuration, in which each body is held at temperature T_i ($i = 1, 2, 3$). As far as the material properties of the three slabs are concerned, we describe them in terms of three complex dielectric permittivities $\varepsilon_i(\omega)$, meaning that their electromagnetic response is local and nonmagnetic.

Herein we are interested in comparing the heat flux on body 3 in two- and three-body configurations. The heat-transfer problem in the case of a couple of arbitrary bodies in a thermal environment has been recently solved [21]. In this case, the heat flux on a body can be expressed as a sum of an evanescent and a propagative contribution: the former (the latter) depends only on the modes of the electromagnetic field for which the transverse wave vector $\mathbf{k}$ satisfies $ck > \omega$ ($ck < \omega$). The evanescent contribution, only connected to the temperatures T_1 and T_3 of the two bodies, largely dominates on the propagative one at distances between them smaller than the thermal wavelength (some microns at ambient temperature). In this near-field regime the monochromatic heat flux on body 3 at frequency ω can be written under the form of a Landauer expansion

$$\phi_{2s}(\omega, d) = \hbar\omega n_{13}(\omega)\sum_p \int_{ck>\omega} \frac{d^2\mathbf{k}}{(2\pi)^2}\mathcal{T}_{2s,p}(\omega, \mathbf{k}, d) \tag{2}$$

where

$$\mathcal{T}_{2s,p}(\omega, \mathbf{k}, d) = \frac{4\mathrm{Im}(\rho_{1p})\mathrm{Im}(\rho_{3p})e^{-2\mathrm{Im}(k_z)d}}{|1 - \rho_{1p}\rho_{3p}e^{-2\mathrm{Im}(k_z)d}|^2}. \tag{3}$$

These quantities depend also on the thicknesses of slabs 1 and 3 through the reflection coefficients ρ_i of slab i [22].

The scattering procedure developed to investigate heat and momentum transfer between two bodies described detail in Ref. [21] has been generalized to the case of three bodies in a thermal environment [23]. In this case, as expected on physical grounds, the evanescent contribution

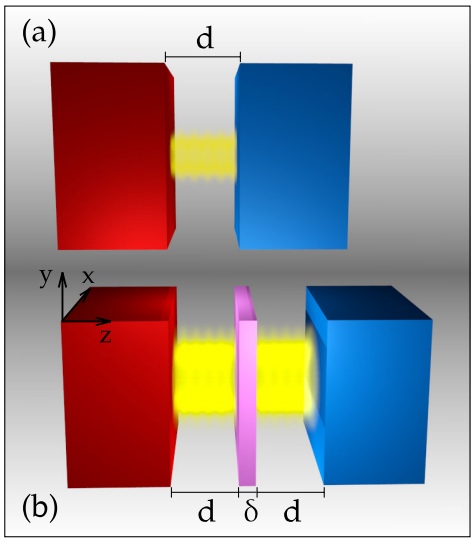

FIG. 1 (color online). Geometry of the system in the (a) two- and (b) three-slab configurations. The distance d between adjacent slabs (1–2 and 2–3) in the three-body configuration equals the distance between slabs in the two-body case.

is a function of the three temperatures T_1, T_2, and T_3, while the environmental temperature T_e enters only in the propagative term. In order to reduce the number of free parameters for the analysis of the amplification mechanism, we will focus our attention on the symmetric case in which the distances between adjacent slabs in the three-body configuration (1–2 and 2–3) are both equal to d, i.e., the distance between slabs 1 and 3 in the two-body configuration (see Fig. 1). This choice makes d the only relevant distance in both scenarios. Moreover, it makes the minimal distance between any couple of adjacent bodies the same for the two configurations and the optical distance between slabs 1 and 3 *double* in the three-slab case with respect to two slabs. For the three-slab system the near-field expression of the monochromatic heat flux on slab 3 reads [23]

$$\begin{aligned}\phi_{3s}(\omega, d, \delta) = \hbar\omega\sum_p \int_{ck>\omega} \frac{d^2\mathbf{k}}{(2\pi)^2} \\ \times [n_{12}(\omega)\mathcal{T}^{(12)}_{3s,p}(\omega, \mathbf{k}, d, \delta) \\ + n_{23}(\omega)\mathcal{T}^{(23)}_{3s,p}(\omega, \mathbf{k}, d, \delta)]\end{aligned} \tag{4}$$

with

$$\begin{aligned}\mathcal{T}^{(12)}_{3s,p}(\omega, \mathbf{k}, d, \delta) \\ = \frac{4|\tau_{2p}(\delta)|^2\mathrm{Im}(\rho_{1p})\mathrm{Im}(\rho_{3p})e^{-4\mathrm{Im}(k_z)d}}{|1 - \rho_{12p}(\delta)\rho_{3p}e^{-2\mathrm{Im}(k_z)d}|^2|1 - \rho_{1p}\rho_{2p}(\delta)e^{-2\mathrm{Im}(k_z)d}|^2} \\ \mathcal{T}^{(23)}_{3s,p}(\omega, \mathbf{k}, d, \delta) = \frac{4\mathrm{Im}[\rho_{12p}(\delta)]\mathrm{Im}(\rho_{3p})e^{-2\mathrm{Im}(k_z)d}}{|1 - \rho_{12p}(\delta)\rho_{3p}e^{-2\mathrm{Im}(k_z)d}|^2}.\end{aligned} \tag{5}$$

In the right-hand side of Eq. (4) the dependence on the couple $(\omega, \mathbf{k})$ is implicit. We note that the evanescent term

splits into two contributions, associated to the couples of temperatures (T_1, T_2) and (T_2, T_3), each one containing a different Landauer transmission probability which is weighted using the corresponding difference $n_{ij}(\omega)$ of thermal populations. The amplitudes (5) contain the transmission amplitude τ_2 of slab 2 and the reflection amplitude associated to the couple of slabs (1,2) treated as a unique body, taking the form [for a given couple $(\omega, \mathbf{k})$],

$$\rho_{12p}(\delta) = \rho_{2p}(\delta) + \frac{\tau_{2p}^2(\delta)\rho_{1p}e^{-2\mathrm{Im}(k_z)d}}{|1 - \rho_{1p}\rho_{2p}(\delta)e^{-2\mathrm{Im}(k_z)d}|^2}. \quad (6)$$

The expressions (5) and (6) depend on the thickness δ of the intermediate slab exclusively through the reflection and transmission coefficients ρ_{2p} and τ_{2p} of slab [22].

Let us now consider the choice of temperatures. To avoid the introduction of a supplementary thermal source and thus keep the comparison between the two configurations meaningful we choose for T_2 the value such that the heat flux on body 2 is zero. In the particular case of a quasimonochromatic flux at frequency ω_{spp} (quite accurate in the near-field regime, as we will see) it can be shown [22] that T_2 is the solution of $2n(\omega_{\mathrm{spp}}, T_2) = n(\omega_{\mathrm{spp}}, T_1) + n(\omega_{\mathrm{spp}}, T_3)$. For the present calculation we take $T_1 = 400$ K and $T_3 = 300$ K, resulting in $T_2 \simeq 357$ K. Finally, we discuss the material properties of the three slabs. As for media 1 and 3, we have chosen two SiC slabs of thickness 5 μm. As for the intermediate slab, it is a metallicke medium described by a simple Drude model $\varepsilon(\omega) = 1 - \omega_P^2/\omega(\omega + i\gamma_P)$, defined by a plasma frequency ω_P and a relaxation rate γ_P. As it is well known [24], this model predicts the existence of a surface mode, a plasmon, at a frequency close to $\omega_P/\sqrt{2}$. Hence, a natural choice for ω_P to maximize heat transfer is $\omega_P = \sqrt{2}\omega_{\mathrm{spp}}$, $\omega_{\mathrm{spp}} \simeq 1.787 \times 10^{14}$ rad s^{-1} being the surface plasmon-polariton frequency supported by SiC, matching the SiC and Drude surface-polariton frequencies.

We are now ready to calculate the ratio between the total heat flux on slab 3 in the three-slab case with respect to the two-slab configuration. Figure 2 shows this ratio for distances $d \in [50, 800]$ nm and thicknesses of the central slab $\delta \in [0, 1]$ μm. This figure clearly shows the existence of a region of parameters in which the three-body heat flux is larger than its two-body counterpart. Concerning the value of the amplification, in our physical configuration it reaches 60% for short distances (around 150 nm). As shown in the inset of Fig. 2, the amplification effect is robust with respect to the relaxation rate γ_P over a range going up to values typical of metals. Moreover, the amplification exists up to distances around 650 nm and, for each value of d, is limited to a finite interval of δ. More in detail, for a given d, we see that the amplification assumes a maximum for $\delta \simeq d$.

In order to get insight on this amplification mechanism, we first analyze the flux spectra $\phi_{2s}(\omega, d)$ and $\phi_{3s}(\omega, d, \delta)$ for

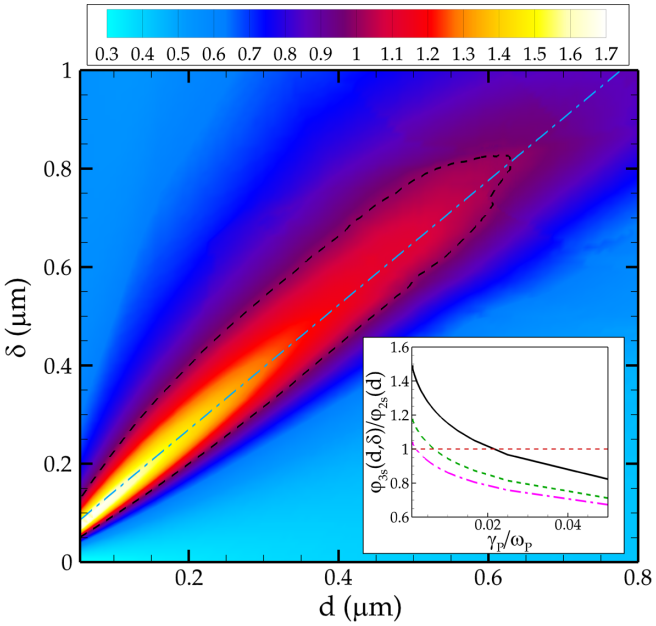

FIG. 2 (color online). Total heat-flux amplification $\varphi_{3s}(d, \delta)/\varphi_{2s}(d)$ as a function of distance and slab thickness. The black dashed line corresponds to $\varphi_{3s}(d, \delta)/\varphi_{2s}(d) = 1$. The dielectric permittivity of SiC is described using a Drude-Lorentz model [25], and for slab 2 we have chosen $\gamma_P = 10^{-3}\omega_P$. The inset shows the dependence of amplification rates on the relaxation rate γ_P for $d = 200$ nm (black solid line), $d = 400$ nm (green dashed line) and $d = 600$ nm (purple dot-dashed line). For each value of d the associated optimal value of δ has been used, respectively, $\delta = 265$, 53, and 755 nm. In the region of amplification, the curve $\delta = 0.014$ nm $+ 1.267d$ (light blue dot-dashed line in the main part of the figure) reasonably describes the dependence of the optimal value of δ with respect to d.

different values of d and for the associated optimal value of δ. The results plotted in Fig. 3 show that when the distance between the two slabs approaches zero, the flux tends to become monochromatic at the surface-polariton frequency. As for the three-slab term, we see that in both cases the spectral component of the flux at ω_{spp} is enhanced with respect to the two-body case. Nevertheless, the presence of slab 2 does not amplify the contribution at smaller frequencies, providing on the contrary a quasimonochromatic enhancement around the surface-polariton frequency ω_{spp}. This explains why, when increasing d, the amplification is less important and eventually the flux ratio goes below one.

This behavior can be understood by looking at the mode coupling efficiencies (3) and (5). We remark that in the two- and three-body configurations the transmission probabilities are multiplied by different weighting functions n_{ij}. In the two-body case, this weight is the difference n_{13}, while n_{12} and n_{23} appear in presence of three slabs. However, due to the quasimonochromaticity of the flux, the temperature T_2 is such that $n_{12}(\omega_{\mathrm{spp}}) = n_{23}(\omega_{\mathrm{spp}}) = n_{13}(\omega_{\mathrm{spp}})/2$. Hence, we compare the transmission probability $\mathcal{T}_{2s}$ with $\mathcal{T}_{3s} = (\mathcal{T}_{3s}^{(12)} + \mathcal{T}_{3s}^{(23)})/2$.

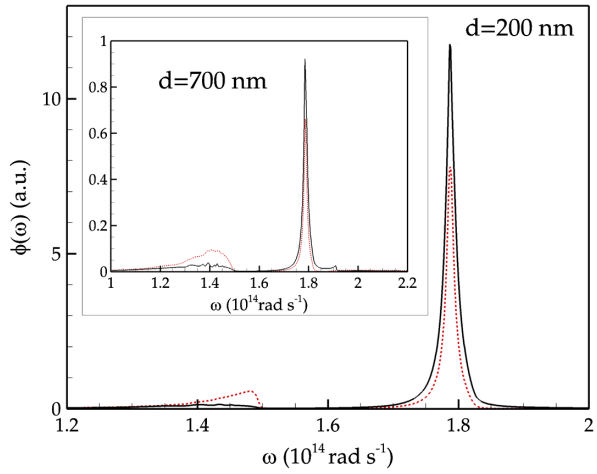

FIG. 3 (color online). Monochromatic fluxes $\phi_{2s}(\omega, d)$ (red dashed line) and $\phi_{3s}(\omega, d, \delta)$ (black solid line) in arbitrary units for two different values of d. For each distance the associated optimal value of δ has been used ($\delta = 265$ nm and $\delta = 870$ nm, respectively).

These quantities are plotted in Fig. 4 for $\omega = \omega_{\rm spp}$ and $d = 200$ nm, as a function of the wave vector k and thickness δ. We consider only TM polarization, giving the main contribution to the heat transfer [22]. Let us first discuss in Fig. 4(b) the two limiting regimes with respect to δ. For $\delta = 0$ the system reduces to two SiC slabs separated by a distance $2d$. By comparing this case to the two-slab configuration at distance d in Fig. 4(a) we observe a shift of the peak and of the cutoff wave vector k_c, associated to the difference of distance from d to $2d$. Otherwise, when the thickness δ is larger than d, $\mathcal{T}_{3s}$ becomes independent on δ, corresponding to the fact that the slab 2 is seen as semi-infinite. In this limit, Fig. 4(b) shows that the replacement of the SiC slab 1 with a semi-infinite metallic slab produces a shift of k_c toward larger values. This is consistent with the fact that k_c is an increasing function of $1/\sqrt{\mathrm{Im}(\varepsilon_1)\mathrm{Im}(\varepsilon_2)}$ and that at the plasmon frequency $\omega_{\rm spp}$ the imaginary part of the Drude dielectric permittivity is smaller than the one of the Drude-Lorentz model describing SiC. Despite this shift, the integral over k (i.e., the monochromatic flux) is still smaller than in the case of two slabs at distance d. This is a direct consequence of the fact that $T_2 < T_1$.

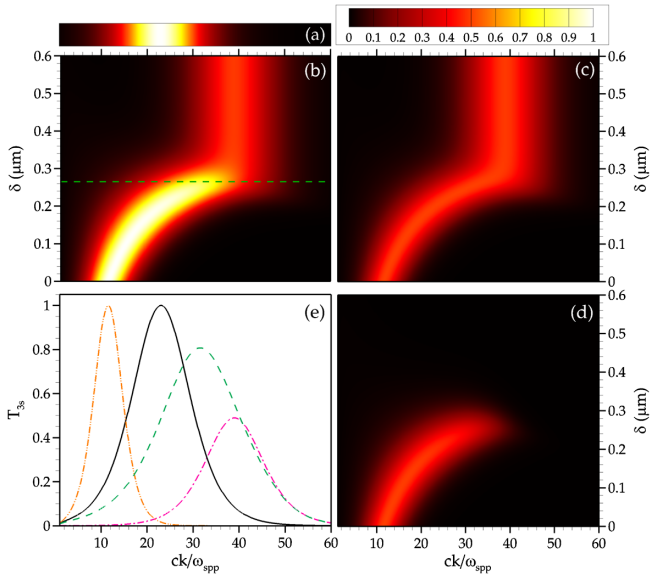

FIG. 4 (color online). Transmission probabilities of a three-body SiC-Drude-SiC system for $\omega = \omega_{\rm spp}$ and $d = 200$ nm as a function of dimensionless wave vector $ck/\omega_{\rm spp}$ and thickness δ. (a) $\mathcal{T}_{2s}$; (b) $\mathcal{T}_{3s} = 0.5(\mathcal{T}_{3s}^{(12)} + \mathcal{T}_{3s}^{(23)})$; (c) $0.5\mathcal{T}_{3s}^{(23)}$; (d) $0.5\mathcal{T}_{3s}^{(12)}$; (e) Three-slab transmission probabilities for $\delta = 0$ nm (orange double-dot-dashed line), $\delta = 265$ nm [optimal thickness, green dashed line, same in panel (b)], and $\delta \to +\infty$ (purple dot-dashed line) compared to the two-slab transmission coefficient (black solid line).

Hence, we can say that the cases $\delta = 0$ and $\delta \gg d$ are as a matter of fact two-body configurations (SiC-SiC and Drude-SiC, respectively). The intermediate region, corresponding to values of δ around d, results from a purely three-body effect in which the results are intimately connected to the presence of both bodies 1 and 2. A deeper understanding of this transition comes from Figs. 4(c) and 4(d), representing separately the two contributions to the three-slab configuration $0.5\mathcal{T}_{3s}^{(23)}$ and $0.5\mathcal{T}_{3s}^{(12)}$, respectively. The former has exactly the structure of a two-body transmission amplitude, as evident from the comparison between (3) and (5). It corresponds to the exchange between the couple (1,2) treated as a unique body at temperature T_2 and the body 3. The plot of this coefficient in Fig. 4(c) shows that this term can be associated to the transition, as a function of δ, from body 2 to body 1. The range of wave vectors contributing to the effect moves from the one associated to a Drude material at distance d to the one corresponding to a SiC slab at distance $2d$. On the contrary, the contribution $\mathcal{T}_{3s}^{(12)}$ can be thought of as an exchange between bodies 1 and 3 mediated by the presence of body 2. The presence of the intermediate slab is manifest both in the temperature-dependent term $n_{12}(\omega)$ and in the fact that the product of the imaginary part of reflection coefficients ρ_1 and ρ_3 is weighted over a coefficient dependent on body 2 and in particular proportional to $|\tau_2|^2$. This explains why this term starts contributing below a given value of δ (around 300 nm in the figure), at which the slab 2 is no longer seen as semi-infinite. In proximity of this value the system exploits the shift of the cutoff k_c due to the replacement of the SiC with the Drude material and at the same time the contribution for smaller wave vectors guaranteed by the presence of slab 1. This is even more evident in Fig. 4(e). In this case we represent the two-slab configuration at distance d, and the three-slab cases for $\delta = 0$, $\delta \gg d$, and $\delta = 265$ nm, representing in this case the optimal value. The curve corresponding to this value of δ shares the behavior for $k \to \infty$ with the case $\delta \gg d$, but differs from this curve at smaller values of k.

In conclusion, we have proposed and characterized a new passive amplifier based on a three-body assisted tunneling mechanism. By remarkably enhancing near-field exchanges with respect to a two-body system, it allows us at the same time to increase the magnitude of heat transfer and to double the separation distance, without any additional source of energy. Due to its quasimonochromaticity and filtering effect, this mechanism could also be exploited to considerably improve the efficiency of near-field energy conversion devices by increasing the photocurrent generation in thermophotovoltaic cells, as well as reducing the heating of the cell. This work also paves the way to the study of near-field heat transport in complex plasmonic systems mediated by many-body interactions at mesoscopic scale.

The authors thank S.-A. Biehs and D. Felbacq for fruitful discussions. M. A. acknowledges financial support from the Julian Schwinger Foundation. P. B.-A. acknowledges the support of the Agence Nationale de la Recherche through the Source-TPV Project No. ANR 2010 BLANC 0928 01.

*riccardo.messina@institutoptique.fr
†mauro.antezza@univ-montp2.fr
‡pba@institutoptique.fr

[1] K. Joulain, J.-P. Mulet, F. Marquier, R. Carminati, and J.-J. Greffet, Surf. Sci. Rep. **57**, 59 (2005).
[2] A. I. Volokitin and B. N. J. Persson, Rev. Mod. Phys. **79**, 1291 (2007).
[3] A. Kittel, W. Müller-Hirsch, J. Parisi, S.-A. Biehs, D. Reddig, and M. Holthaus, Phys. Rev. Lett. **95**, 224301 (2005).
[4] L. Hu, A. Narayanaswamy, X. Chen, and G. Chen, Appl. Phys. Lett. **92**, 133 106 (2008).
[5] E. Rousseau, A. Siria, G. Jourdan, S. Volz, F. Comin, J. Chevrier, and J.-J. Greffet, Nat. Photonics **3**, 514 (2009).
[6] S. Shen, A. Narayanaswamy, and G. Chen, Nano Lett. **9**, 2909 (2009).
[7] T. Kralik, P. Hanzelka, V. Musilova, A. Srnka, and M. Zobac, Rev. Sci. Instrum. **82**, 055106 (2011).
[8] R. S. Ottens, V. Quetschke, S. Wise, A. A. Alemi, R. Lundock, G. Mueller, D. H. Reitze, D. B. Tanner, and B. F. Whiting, Phys. Rev. Lett. **107**, 014301 (2011).
[9] R. S. DiMatteo, P. Greiff, S. L. Finberg, K. A. Young-Waithe, H. K. H. Choy, M. M. Masaki, and C. G. Fonstad, Appl. Phys. Lett. **79**, 1894 (2001).
[10] A. Narayanaswamy and G. Chen, Appl. Phys. Lett. **82**, 3544 (2003).
[11] W. Srituravanich, N. Fang, C. Sun, Q. Luo, and X. Zhang, Nano Lett. **4**, 1085 (2004).
[12] Y. De Wilde, F. Formanek, R. Carminati, B. Gralak, P.-A. Lemoine, K. Joulain, J.-P. Mulet, Y. Chen, and J.-J. Greffet, Nature (London) **444**, 740 (2006).
[13] A. C. Jones and M. B. Raschke, Nano Lett. **12**, 1475 (2012).
[14] P. Ben-Abdallah and K. Joulain, Phys. Rev. B **82**, 121419 (2010).
[15] S.-A. Biehs, E. Rousseau, and J.-J. Greffet, Phys. Rev. Lett. **105**, 234301 (2010).
[16] R. Landauer, Philos. Mag. **21**, 863 (1970).
[17] M. Büttiker, Phys. Rev. Lett. **57**, 1761 (1986).
[18] J. B. Pendry, J. Phys. Condens. Matter **11**, 6621 (1999).
[19] P. Ben-Abdallah, S.-A. Biehs, and K. Joulain, Phys. Rev. Lett. **107**, 114301 (2011).
[20] Z. H. Zheng and Y. M. Xuan, Nanoscale Micro. Thermophys. Eng. **15**, 237 (2011).
[21] R. Messina and M. Antezza, Europhys. Lett. **95**, 61 002 (2011); Phys. Rev. A **84**, 042102 (2011).
[22] See Supplemental Material at http://link.aps.org/supplemental/10.1103/PhysRevLett.109.244302 for the definition of reflection and transmission coefficients, a discussion concerning the value of T_2, as well as a brief description of the modes in the three-slab configuration.
[23] R. Messina and M. Antezza (to be published).
[24] E. N. Economou, Phys. Rev. **182**, 539 (1969).
[25] *Handbook of Optical Constants of Solids*, edited by E. Palik (Academic Press, New York, 1998).